Voltammetric Behavior of Zinc Hexacyanoferrate (III) Nanoparticles and Their Application in the Detection of N-Acetylcysteine

Vanessa Solfa dos Santos[1], Vitor Alexandre Maraldi[1], Kely Silveira Bonfim[1], Tamires Rocha Souza[1], Ana Paula Rizzato Nakamura[1], Maiara de Souza Magossi[1], Mariana de Souza Magossi[1], Daniela Silvestrini Fernandes[1], Devaney Ribeiro do Carmo[1*]

Faculdade de Engenharia de Ilha Solteira UNESP – Universidade Estadual Paulista "Júlio de Mesquita Filho", Departamento de Física e Química, Av. Brasil, 56. CEP 15385-000, Ilha Solteira, SP, Brazil. Fax: (+55 18) 3742-4868.
*E-mail: docarmo@dfq.feis.unesp.br

The present work reports the voltammetric behavior of Zinc hexacyanoferrate (III) nanoparticles and their application in the detection of N-acetylcysteine. Two distinct ratios of water/formamide 10:0 (ZnH-1) and 4:6 (ZnH-2) were studied in the complexation reaction of Zn^{2+} with $[Fe^{III}(CN)_6]^{3-}$. The materials were characterized by Transmission Electron Microscopy (TEM) and Cyclic Voltammetry. The cyclic voltammograms of ZnH-1 and ZnH-2 showed a well-defined redox couple with formal potential $(E^{\theta'})$ = 0.94 ± 0.01 V (ν=20 mVs^{-1}; KCl 1.0 M)) attributed to the redox process $[Fe^{II}(CN)_6]/[Fe^{III}(CN)_6]$ in the presence of Zn^{2+}. The graphite paste electrode modified with ZnH-1 and ZnH-2 presents a sensitive and catalytic oxidation response for the determination of N-acetylcysteine respectively.

1. INTRODUCTION

Currently, the preparation of metal nanoparticles has attracted increasing attention in materials chemistry due the possibility to arouse emerging physical (magnetic, electrical or optical) or chemical (catalytic-electrocatalytic) properties that are dependent on particle size [1-8]. Various methods for synthesizing metal NPs were recently reviewed by Rotemberg [9,10]. Generally, metal nanoparticles tend to agglomerate and, because of their small size, they become difficult to re-disperse. [3]. To avoid

these disadvantages, metal nanoparticles are usually loaded on porous supports, which prevents clustering and make their manipulation recovery easier, but this procedure is time consuming and involves several analytical steps.

Metal hexacyanoferrates (MHCFs) are a class of polynuclear inorganic mixed valence compounds with zeolitic nature, exhibiting excellent redox and high ionic conductivity properties [11,12]. These materials have exciting applications in different fields such as electro-chromism, electrocatalysis, electro analytical applications [13], solid state batteries [14-16] and photo image formation [17,18]. Nanoparticles of metal hexacyanoferrates (MHCFs) have been prepared by a diversity of methods [19,20]. For the nanoparticle synthesis it has also been employed various stabilizing agents such as ionic liquids, capping ligands or porous matrices, like biopolymer chitosan or mesostructured silica to obtain NPs in solution or as nanocomposites [21]. The stabilizing agent serves to prevent aggregation and to mediate the size of PB NPs [22-24].

MHCFs nanoparticles generally have a high surface area and well-defined redox process therefore suitable to function as electron mediators in catalytic oxidation processes increasing the deployment of electrochemical sensors for detection of various organic and inorganic molecules.

In this work we report an approach for the preparation of zinc hexacyanoferrate nanoparticles from a mixture of water and formamide. Zinc hexacyanoferrate exhibits well-defined and reproducible electrochemical responses, because both the oxidized and reduced structures of ZnHCF are fairly open and permit transport of alkali metal counter cation providing charge balance during redox transitions.

From the electrochemical aspect among the metal hexacyanoferrates, zinc hexacyanoferrate (ZnHCF) requires further studies, for the reason that it is not readily deposited on surfaces like platinum (Pt), glassy carbon (GC) and gold (Au) [25]. As an insoluble powder, it does not have much information regarding their use as an electrochemical sensor or voltammetric behavior [25-27].

The method presented here is to obtain a nano-sized zinc hexacyanoferrate (III) without any template and with a high potential to function as electrochemical sensor. After a detailed voltammetric study the ZnHCF nanoparticles were tested to a simple and fast voltammetric detection of N-acetylcysteine, using graphite paste electrode.

2. EXPERIMENTAL

2.1. Reagents and Solutions

All reagents (zinc chloride, potassium hexacyanoferrate (III), N-acetylcysteine and supporting electrolytes) and solvents (formamide) used were of analytical grade (Alpha Aesar, Merck or Aldrich). All solutions (N-acetylcysteine) and supporting electrolytes (KCl, NaCl, LiCl, NH$_4$Cl) were prepared using deionized water was obtained using a Milli-Q Gradient system from Millipore was used. The solutions of N-acetylcysteine were prepared immediately before use.

2.2. Preparation of Nanoparticles of Zinc Hexacyanoferrate(III)

For the synthesis of the nanoparticles was used a procedure described in the literature [28], with some modifications and described as follows [29]: two solutions, A and B, were prepared, solution A consisting of 2.13×10^{-3} mol of $K_3[Fe(CN)_6]$ dissolved in 30 mL of water and formamide mixture. Solution B was prepared by dissolving 2.72×10^{-3} mol of $ZnCl_2$ in 20 mL of water and formamide. After solution was prepared, the solution A was poured into solution B and stirred for 2 hours. The solid phase was isolated by centrifugation (1.500 rpm). Then the solid phase was filtered and washed exhaustively with distilled water thoroughly to eliminate the potassium chloride formed during the reaction. The materials were dried at 60°C. The effect of formamide on the synthesis was investigated through the synthesis of two samples, ZnH-1 and ZnH-2, using two reaction media with different volume ratios of water and formamide to be 10:0; 4:6 ratios respectively.

2.3. Characterization measurements

The as prepared nanoparticles were morphologically studied by transmission electron microscopy (TEM; Philips, model CM 200) and correlated techniques, such as selected area electron diffraction (SAED). Samples were prepared by dropping two drops of a suspension of nanoparticles in alcohol on a coated Cu grip.

2.4. Electrochemical Measurements

Cyclic voltammograms were performed using the Microquimica (MQP1- PGST) potentiostat. The three electrode systems used in these studies consisted of a modified working electrode (graphite paste electrode), an Ag/AgCl reference electrode, and a platinum wire as the auxiliary electrode. The measurements were carried out at 25°C. The graphite paste electrode modified with ZnH nanoparticles was prepared by mixing 20 mg of ZnH with 90 mg of graphite (Aldrich) and 50 μL of mineral oil. The electrode body was produced from a glass tube of 3 mm i.d. and 14 cm height, containing graphite paste [30, 31].

A copper wire was inserted through the opposite end of the glass tube to establish electrical contact. After homogenizing the mixture, the modified paste was carefully positioned on the tube tip to avoid possible air gaps, which often enhances electrode resistance. The external surface of the electrode was smoothed on soft paper. A new surface can be produced by scraping out the old surface and replacing the graphite paste [30, 31].

3. RESULTS AND DISCUSSION

Zinc Hexacyanoferrate (III) nanoparticles were prepared easily on mixing the solution of zinc ions with the solution of hexacyanoferrate ions from a solution containing water and formamide. Different ratios of water and formamide were tested. The analytical results of both systems (ZnH-1-ZnH-2) revealed that the molecular formula of Zinc hexacyanoferrate (III) were very close, and concluded that the synthesized compounds have a molecular formula of $Zn_3[Fe(CN)_6]_2.nH_2O$ [29].

Equation 1 describes the reaction of prepared zinc hexacyanoferrate nanoparticles.

$$2[Fe(CN)_6]^{3-} + 3Zn^{2+} + \text{water or mixture water/formamide)} \rightleftharpoons Zn_3[Fe(CN)_6]_2 \cdot nH_2O \qquad [1]$$
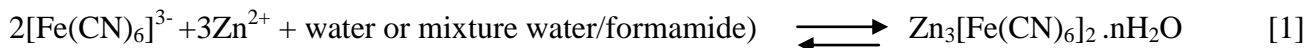
In a previous publication, the ZnH nanoparticles have been well characterized by different techniques [29] but TEM results has not yet been shown. Then TEM was employed here as a complementary characterization, to identify the size and means of prepared zinc hexacyanoferrate nanoparticles (Fig. 1). To ZnH-1 system the transmission electron microscopy (TEM) images of samples show discrete spherical particles with relatively homogeneous size (A). These connected discrete particles were are not well crystalline as observed from selected area electron diffraction (SAED) pattern (C). The ZnH-2 system (B) characterization showed the size ranging around 50 nm and these nanoparticles consist of uniform monodisperse cubic form nanostructures, with slight agglomeration around the cubic nanoparticles. The SAED pattern from the ZnH-2 (D) shown a cube-shaped crystal. The surface electrocatalytic properties of material is highly dependent on its surface area. As shown by Fig. 1(B), It is clear that the nanoparticles in ZnH-2 are more expendable, which implies a larger active surface area.
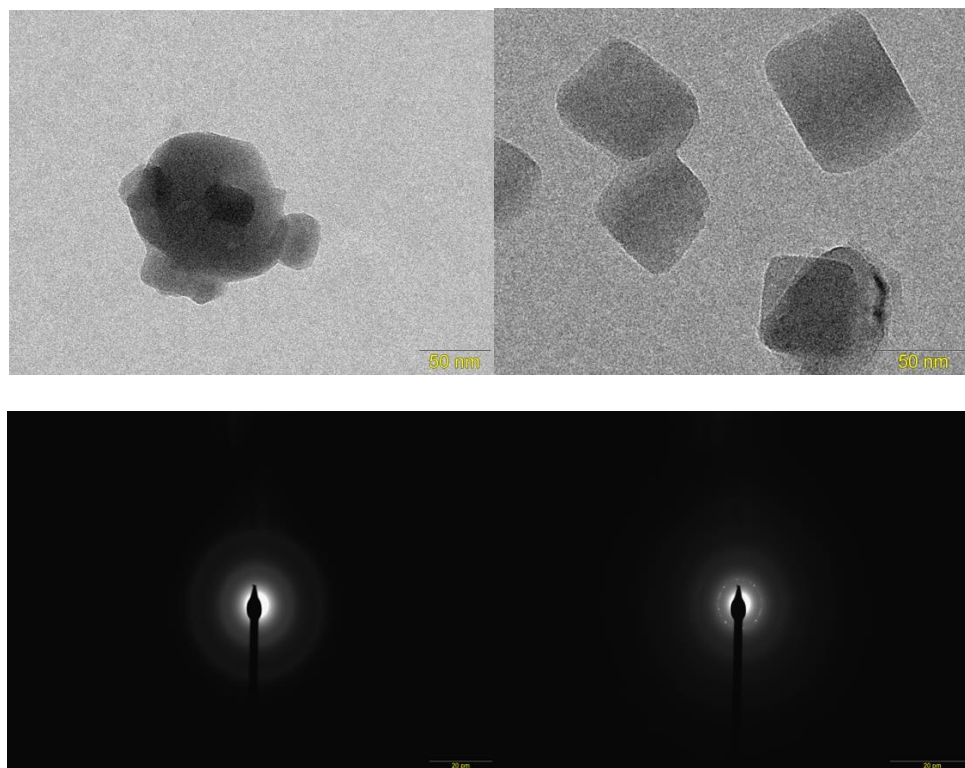
Figure 1. Transmition electron macroscopy (TEM) and selected area electron diffraction (SAED) pattern respectively for the systems: ZnH-1 (A and C); ZnH-2 (B and D).

For the ZnH-1 system the surface area is smaller because the particles are more agglomerated. In this way the difference in nanoparticle dispersion will reflect on the electrocatalytic properties of these materials.

3.3 Electrochemical characterization of ZnH nanoparticles

To two systems, a well-defined redox couple was observed, with formal potential $(E^{\theta'})$ = 0.94 ± 0.01 V (ν = 20 mV s^{-1}; KCl 1.0 M)) ($E^{\theta'}$ = Eap + Ecp / 2; where Eap and Ecp are anodic and cathodic peak potentials) attributed to the redox process $[Fe^{II}(CN)_6]/[Fe^{III}(CN)_6]$ in presence of Zn^{2+}. Voltammetric studies about thin film of Zinc hexacyanoferrate (II) formed directly on a Zn electrode [26] or on the wax impregnated graphite electrode (WIGE) [27] report a formal potential values of 0.666 and 0.630 V (vs SCE) respectively, however the value found in this paper was close to that found for the zinc hexacyanoferrate (II) supported on the titanium dioxide-silica gel composite [32].

3.3.1 Studies on the effect of cations and anions

The process of oxi-reduction of the $Zn_3[Fe(CN)_6]_2 \cdot 2H_2O$ takes place initially by the equilibrium of the cation (alkaly metals salt) present in the support electrolyte with the electrode surface containing the nanoparticles [33, 34]. The nature of cations and anions was observed to affect the formal potential $(E^{\theta'})$ and the intensities of current in the studies performed with different electrolytes tested, as illustrated in Figure 2 to ZnH-1 (A) and ZnH-2 (B) systems. The current intensity and formal potential ($E^{\theta'}$ shifted to more anodic potentials) of redox couple of both, was influenced more drastically by the nature of the cation according to the sequence: $NH_4^+ > K^+ > Na^+$ for both systems. It was possible to observe a better electrochemical response of graphite paste electrode modified with $Zn_3[Fe(CN)_6]_2 \cdot 2H_2O$ nanoparticles in the presence of electrolyte containing the cations K^+ and NH_4^+, as shown in the voltammograms of Figure 2 (line black). The cation K^+ has a better voltammetric performance and in relation to the cation NH_4^+ (same hydrated radius).
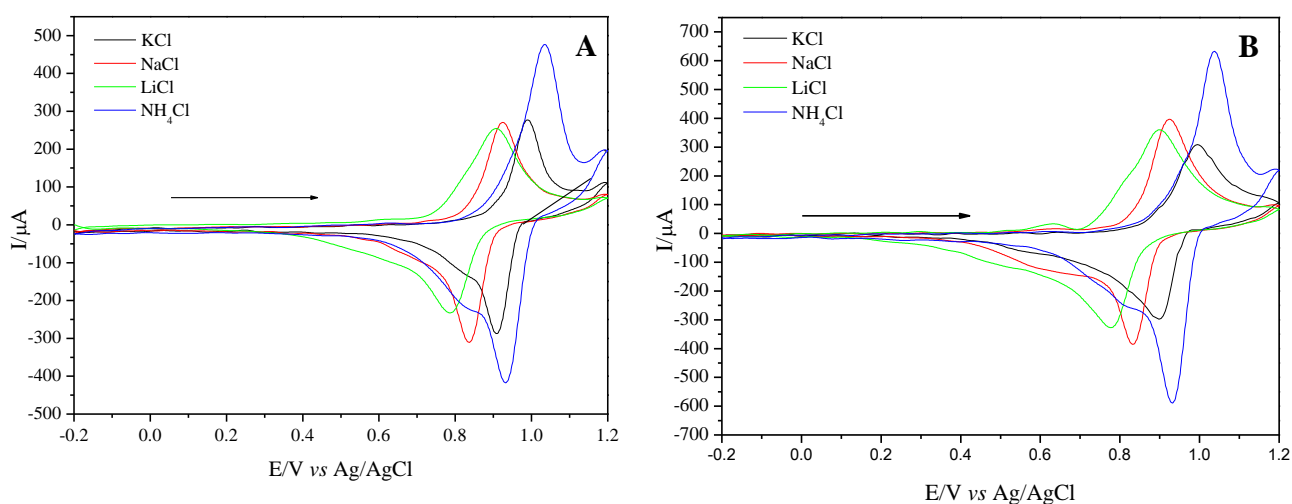
Figure 2. Cyclic voltammograms of graphite electrode modified with ZnH-1 (A) and ZnH-2 (B) in different electrolytes (1.0 mol L^{-1}; ν = 20 mV s^{-1}; 20% (w/w)).

Cyclic voltammograms of the graphite paste electrode modified with $Zn_3[Fe(CN)_6]_2 \cdot 2H_2O$ recorded in presence of different anions indicated that the redox processes are strongly influenced by the nature of the anion (Cl^-, NO_3^-) (results not showed here).

From these studies it is clear that support electrolytes, the base of alkali metal salts play an important role in the electrochemical behavior of Zn-H. The displacement of $E^{\theta'}$ is due to the fact that compounds such as Prussian blue and analogues exhibit structures that have a zeolite cavity, in other words, channels that allow the insertion of small molecules and ions that behave as zeolites [33-35]. The K^+ cation is more easily lodged in the pores of the zeolite structure of the formed ZnH, because having smaller hydrated radius. A shift of $E^{\theta'} = 60$ mV to more positive potentials for the same anion (for example Cl^-), was observed when Na^+ is exchanged for K^+. This increase of $E^{\theta'}$ is not accompanied with the increase of ΔEp, which in this case was of 80 ± 10 mV. All the cations tested showed the presence of only one well-defined redox pair. Because of its good chemical stability and good voltammetric performance besides presenting electrochemical parameters close to reversibility, through this study the KCl could be choosen as the best supporting electrolyte.

Figure 3 shows the cyclic voltammograms recorded at different concentrations of KCl (0.1 to 2.0 M). As expected the cation concentration of the electrolyte supporting electrolyte is involved in the redox couple.
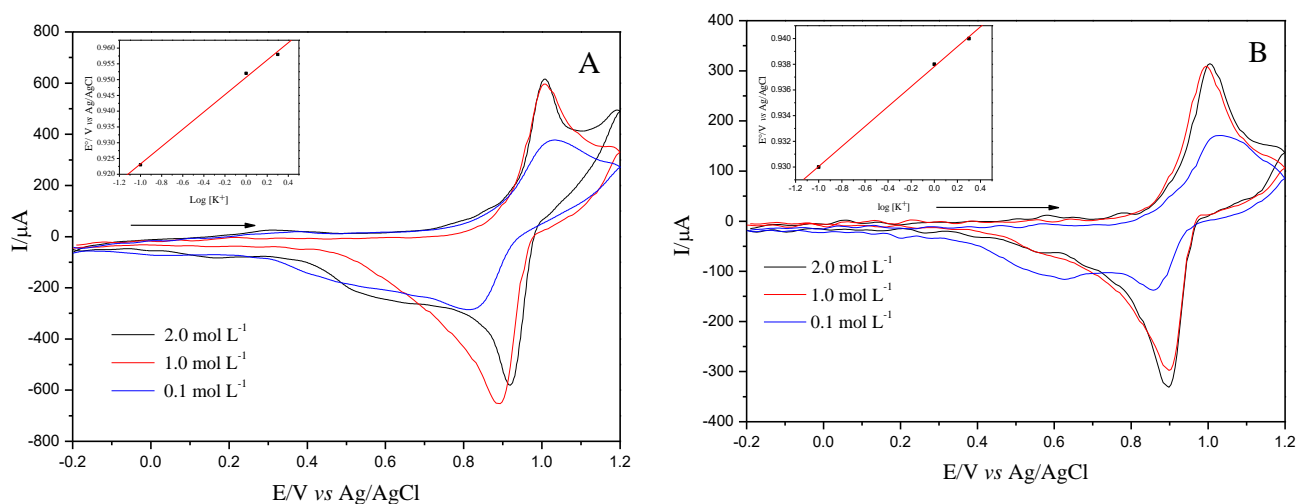
Figure 3. Cyclic voltammograms of the graphite paste electrode modified with ZnH-1 (A) and ZnH-2 (B) at different concentrations (KCl; v = 30 mV s^{-1}; 20% (w/w)). Graphic inserted: ($E^{\theta'}$) of graphite paste modified with ZnH-1 (A) and ZnH-2 (B) as a function of KCl concentration.

The $E^{\theta'}$ moves to more positive values with increasing electrolyte concentration, thus indicating the participation of K^+ ion in the redox process and also a change in the activity of these ions [36, 37]. In both systems the dependence of formal potential versus log K^+ was linear and the slope of the line was 30 mV per decade of K^+ concentration, suggesting a quasi-Nernstian process involving two electrons [38].

The study of the hydrogen ion concentration showed that the formal potential ($E^{\theta'}$) of the two system remained unchanged at pH values between 3 and 9 and practically do not cause any marked

change in the electrochemical parameters of the system. It was observed that the ZnH-1 system showed a sharp shoulder at 0.6 V in the cathodic scan, attributed to cyanide groups protonation.

This is an indicative occurrence of the interaction between the H$^+$ ions with the cyanide groups (protonation) more pronounced in ZnH-1(A) than ZnH-2 (B) system.

Figure 4 illustrates the cyclic voltammogram of ZnH-1 (A) and ZnH-2 (B) systems at different scan rate (10 to 250 mV s^{-1}). It's evident that, with increasing scan rate, there is an increase of anodic and cathodic peak potential and a shift of E$^{\theta'}$ to more positive potential regions. The inserted graph in Fig. 4 shows the linear dependence between the current intensity of the anodic/cathodic peak and the square root of the scan rate for ZnH-1 (A) and ZnH-2 (B) systems, featuring a diffusion process [38].
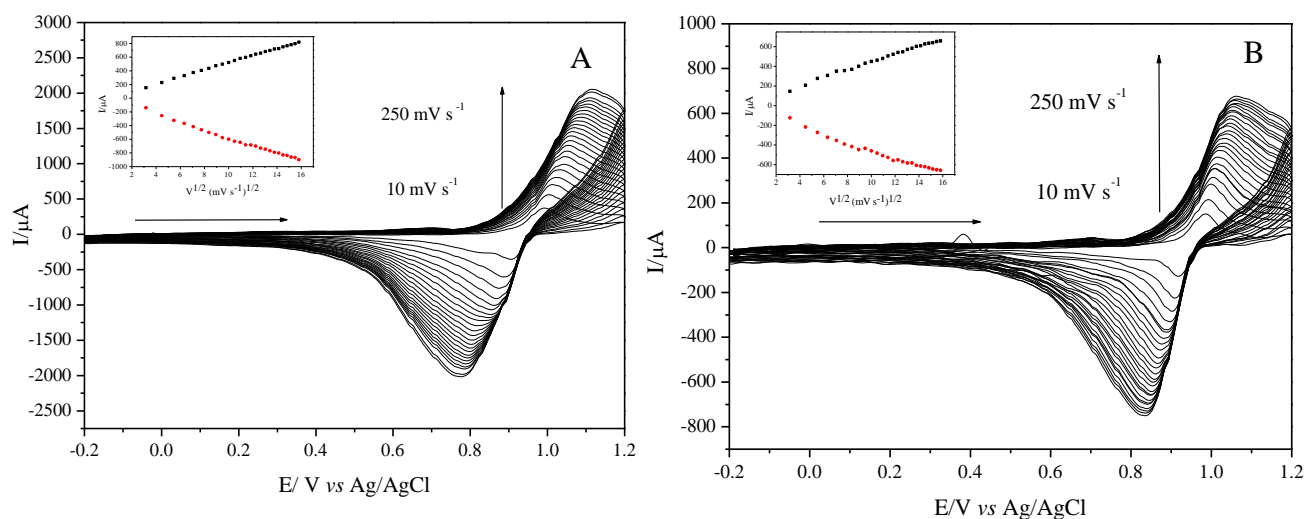
Figure 4. Cyclic voltammograms of ZnH-1 (A) and ZnH-2 (B) at different scan rates (KCl 1.0 mol L^{-1}; 20% (w/w)) (Graphic inserted: dependence of peak current intensity (anodic and cathodic) as a function of square root of scan rate).

The graphite paste electrode modified with ZnH-1 and ZnH-2 presents a sensitive and catalytic oxidation response for the determination of N-acetylcysteine respectively. Figure 5 shows the cyclic voltammograms of the graphite paste electrode in the absence (curve a) and in the presence of N-acetylcysteine (curve c) and the voltammograms of the graphite paste modified with ZnH-1 (A) and ZnH-2 (B) in the absence (curve b) and in the presence of N-acetylcysteine (curve d). This shows a good response from the modified graphite paste electrode for the determination of N-acetylcysteine.

Figure 6 shows the sensitivity of the graphite paste electrode modified with ZnH-1 (A) and ZnH-2 (B) with different additions of aliquots of N-acetylcysteine.

When the N-acetylcysteine concentration was increased, a significant increase in the anodic current peak intensity and also a slight displacement of the formal potential of both peaks to more negative values were observed. It was observed that the electro-oxidation of the N-acetylcysteine was more pronounced for ZNH-2 system, suggesting that formamide plays an important role in the formation and properties of the nanoparticles. This sensitivity presented by the graphite

paste electrode modified with ZnH makes it susceptible to the analysis of millimolar concentration of N-acetylcysteine.
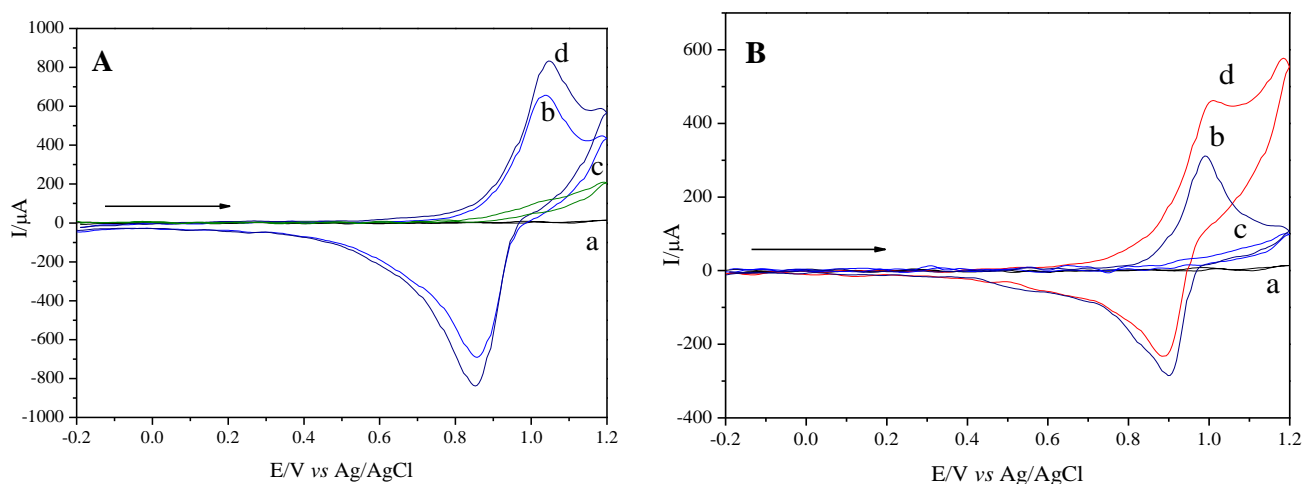
Figure 5. **Cyclic voltammograms for the systems: Zn-H-1 (A); Zn-H-2 (B): (a) graphite paste electrode; (b) modified graphite paste electrode with ZnHCF; (c) graphite paste electrode and aliquot of N-acetylcysteine; (d) modified graphite paste electrode with ZnH and aliquot of N-acetylcysteine (KCl 1.0 mol L^{-1}; 20mV s^{-1}; 20% (w/w)).**
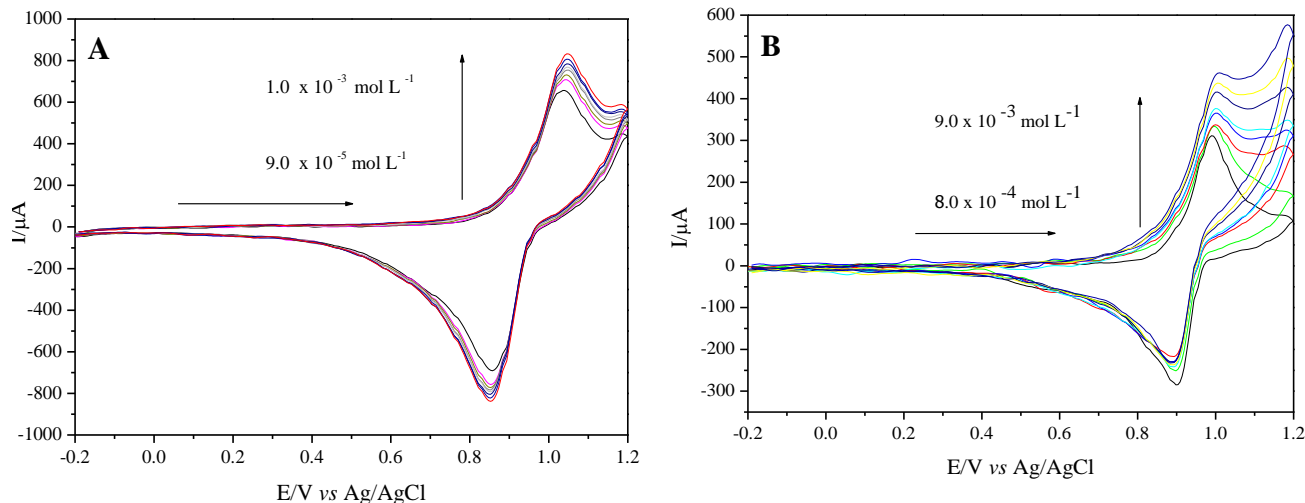
Figure 6. Cyclic voltammograms obtained for the modified graphite paste electrode with in the presence of different N-acetylcysteine concentrations for the following system: ZnH-1 (A) (9.0×10^{-5} to 8.0×10^{-4}); ZnH-2 (B) (8.0×10^{-4} to 9.0×10^{-3} mol L^{-1}) (KCl 1.0 mol L^{-1}; 20mV s^{-1}; 20% (w/w)).

This increased anodic current intensity occurs due to electro-oxidation of the N-acetylcysteine by the mediator ZnH-1. Fe(III) produced during the anodic scanning chemically oxidizes n-acetylcysteine, while this is reduced to Fe(II), which in turn is electrochemically oxidized to Fe(III).

The electro-oxidation of N-acetylcysteine was mediated for ferricyanide (mediator) and occurs for an EC mechanism, where E is the electrochemical step and C is the chemical step.

Thus, N-acetylcysteine oxidized at the electrode surface, and this process occurs at the potential of 0.99 V about 200 mV more positive than previous work [39]. When employing unmodified graphite paste electrode or glassy carbon electrode, the oxidation process does not occur in this potential. It was observed that the catalytic current of N-acetylcysteine in these modified electrodes decreases over time after the first cycle, probably due to decrease [40,41] near the electrode surface or due to the fact that the electrode response is blocked by the product resulting from the reaction [41].

Therefore, in view of this l-cysteine reaction [42], the oxidation of N-acetylcysteine on the electrode surface of the graphite paste electrode modified with ZnH-1 and ZnH-2 can be described by the following chemical equations:

$$K_2 Zn_3^{(II)}[Fe^{(II)}(CN)_6]_2 \rightleftharpoons Zn_3^{(II)}[Fe^{(III)}(CN)_6]_2 + 2K^+ + 2e \quad (E) \qquad [2]$$
$$Zn_3^{(II)}[Fe^{(III)}(CN)_6]_2 + 2K^+ + 2NACySH \rightleftharpoons K_2Zn_3^{(II)}[Fe^{(II)}(CN)_6]_2 + NACyS\text{-}SCy + 2H^+ \qquad [3]$$
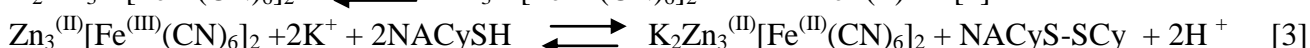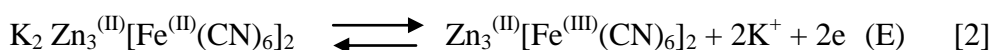
were NACySH is N-acetylcysteine and NACyS-SCy is N-acetylcystine.

It is worth noting that a sensibility was only ZnH-1, when to ZnH-2 was observed a strong electrocatalytic activity. The modified electrode gives a linear range (Figure 7 A and B) from 9.0×10^{-5} to 1.0×10^{-3} mol L^{-1} (R = 0.996) and 8.0×10^{-4} to 9.0×10^{-3} mol L^{-1} (R = 0.997) with detection limit of 4.46×10^{-5} and 2.67×10^{-4} A mol L^{-1} and amperometric sensitivity of 0.132 mA/ mol L-1 and 0.017, respectively for ZnH-1 and ZnH-2 in the N-acetylcysteine detection.
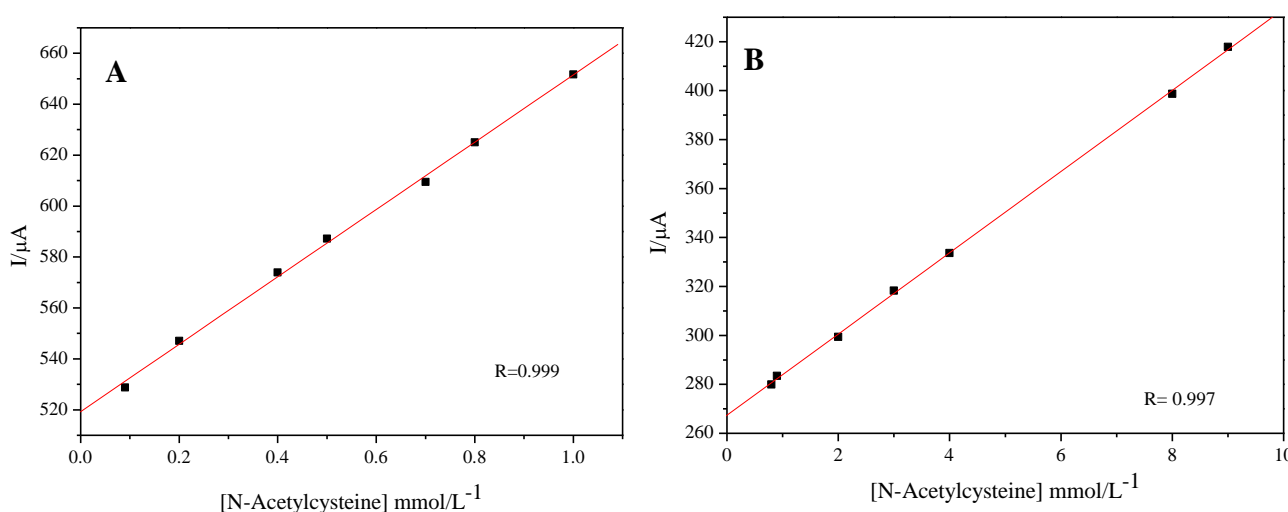
Figure 7. Analytical curve of anodic peak for the determination of N-acetylcysteine using the modified graphite paste electrode with: Zn-H-1 (A); Zn-H-2 (B) (KCl 1,0 mol L^{-1}, pH 7,0; v = 20 mV s^{-1}; 20%(w/w)).

Table 1 list the main electroanalytical parameters obtained for ZnH systems. From the Table 1, it is clear that ZnH-1 system displays a lower detection showed a linear response over a wider concentration range. Amperometric sensitivity for systems ZnH-1 and ZnH-2 were 0.132 and 0.016 A mol L^{-1}.

Table 1. Parameters of the calibration curve for the detection of N-acetylcysteine (N-ac).

System	Linear Range	CC (R) [a]	LOD mol L^{-1} [b]	AS A mol L^{-1} [c]	EC [d]
ZnH-1	9.0×10^{-5} - 1.0×10^{-3}	0.999	4.46×10^{-5}	0.132	$Y(A) = 5.19 \times 10^{-4} + 0.132$ [N-ac]
ZnH-2	8.0×10^{-4} - 9.0×10^{-3}	0.997	2.67×10^{-4}	0.017	$Y(A) = 2.67 \times 10^{-4} + 0.017$ [N-ac]

[a] CC= Correlation Coefficient; [b] LOD = Limit of Detection; [c] AS = Amperometric Sensitivity; [d] EC = Equation Calibration; n=3.

The ZnH-1 system presented the best analytical parameters such as limit of detection, amperometric sensitivity and a better concentration range for a detection of N acetylcysteine as described in Table 1.

Interferences in the determination of 40 ppm N-acetylcysteine using the graphite paste electrode modified with ZnH were examined by testing the effect of several species frequently found with N-acetylcysteine [40]. The corresponding current intensities were compared with those obtained in the absence of each interference compound.

The effect of several organic acids such as citric acid, oxalic acid, ascorbic acid, and glucose, fructose, sucrose and some inorganic ions such as thiosulfate, persulfate, nitrite, acetate, chloride were carried out adding 500 fold of some of the compounds mentioned. To detect N-acetylcysteine using the modified graphite paste electrode, only sulfite and acetate caused a serious negative interference in the electrode response, the other compounds did not show any interference (at 250 fold).

4. CONCLUSIONS

The nanoparticles of zinc hexacyanoferrate(III) ZnH-1 and ZnH-2 exhibits a well-defined redox couple with formal potential $(E^{\theta'}) = 0.94 \pm 0.01$ V ($\nu = 20$ mV s^{-1}; KCl 1.0 M)). The voltammetric study, showed that the formal potential $(E^{\theta'})$ is strong influenced by concentration and electrolyte nature, but the two system remained unchanged at pH values between 3 and 9. The graphite paste electrode modified with ZnH-1 and ZnH-2 presents a sensitive and catalytic oxidation response for the determination of N-acetylcysteine respectively. The modified graphite paste electrode gives a linear range from 9.0×10^{-5} to 1.0×10^{-3} mol L^{-1} (R = 0.996) and 8.0×10^{-4} to 9.0×10^{-3} mol L^{-1} (R = 0.997) with detection limit of 4.46×10^{-5} and 2.67×10^{-4} A mol L^{-1} and amperometric sensitivity of 0.132

mA/ mol L^{-1} and 0.017, respectively for ZnH-1 and ZnH-2 in the N-acetylcysteine detection. Under these circumstances, the nanoparticles of ZnH can be used for voltammetric detection of N-acetylcysteine.

References

1. J. Garcia-Martinez, N. Linares, S. Sinibaldi, E. Coronado and A. Ribera, *Micropor. Mesopor. Mat.,* 117 (2009) 170.
2. D. R. Do Carmo, M. M. Souza, U. O. Bicalho, V. S. Dos Santos, J. P. Souza and D. R. Silvestrini, *J. Nanomater.,* 2015 (2015) 1.
3. E. Roduner, *Nanoscopic Materials Size-Dependent Phenomena*. RSC Nanoscience & Nanotechnology, Cambridge (2006).
4. M. Hou, Q. Mei and B. Han, *J. Colloid Interface Sci.,* 449 (2015) 488.
5. Y. Zhang, X. Cui, F. Shi and Y. Deng, *Chem. Rev.,* 112 (2012) 2467.
6. H. Liu, T. Jiang, B. Han, S. Liang and Y. Zhou, *Science,* 326 (2009) 1250.
7. C. N. R. Rao, A. Müller and A.K. Cheetham, *The Chemistry of Nanomaterials,*Wiley-VCH, Weinheim (2004).
8. G. Ozin and A. Arsenault, *Nanochemistry: A Chemical Approach to Nanomaterials*, RSC Nanoscience & Nanotechnology, Cambridge, (2005).
9. L. D. Pachón and G. Rothenberg, *Appl. Organomet. Chem.,* 22 (2008) 288.
10. L. D. Marks and L. Peng, *J. Phys. Condens. Matter.,* 28 (2016) 1.
11. P. Wu, S. Lu and C. Cai, *J. Electroanal. Chem*., 569 (2004) 143.
12. S. S. Narayanan and F. Scholz, *Electroanal*., 11 (1999) 465.
13. K. Itaya, I. Uchida and V. D. Neff, *Acc. Chem. Res*., 19 (1986) 162.
14. M. Kaneko and T. Okada, *J. Electroanal. Chem.,* 255 (1988) 45.
15. S. Kalwellis-Mohn and E. W. Grabner, *Electrochim. Acta,* 34 (1989) 1265.
16. M. Jayalakshmi and F. Scholz, *J. Power Sources,* 91 (2000) 217
17. M. Nishizawa, S. Kuwabata and H. Yoneyama, *J. Electrochem. Soc*., 143 (1996) 3462.
18. Y. Wu, B. W. Pfenning and A. B. Bocarsly, *Inorg. Chem,*. 34 (1995) 4262.
19. L. Catala, C. Mathonie`re, A. Gloter, O. Stephan, T. Gacoin, J.-P. Boilot and T. Mallah, *Chem. Commu.,* 6 (2005) 746.
20. T. Uemura, M. Ohba and S. Kitagawa, *Inorg. Chem.,* 43 (2004) 7339.
21. J. Larionova, Y. Guari, C. Sangregorio and C. Guérin, *New J. Chem.,* 33 (2009) 1177.
22. G. Fu, W. Liu, S. Feng and X. Yue, *Chem. Commun.,* 48 (2012) 11567.
23. J. F. Zhai, Y. M. Zhai, D. Wen and S. J. Dong, *Electroanalysis,* 21 (2009) 2207.
24. M. Shokouhimehr, E. S. Soehnlen, J. H. Hao, M. Griswold,C. Flask, X. D. Fan, J. P. Basilion, S. Basu and S. P. D. Huang, *J . Mater. Chem.,* 20 (2010) 5251.
25. V. Jassal, U. Shanker, B. S. Kaith and S. Shankar, *RSC Adv.,* 5 (2015) 26141.
26. A Eftekhari, *J. Electroanal. Chem.,* 537 (2002) 59.
27. J. Joseph, H. Gomathi and G. P. Rao, *J. Electroanal. Chem.,* 431 (1997) 231.
28. V. Vo, M. N. Van, H. I. Lee, J. M. Kim, Y. Kim and S. J. Kim, *Mater. Chem. Phys.,* 107 (2008) 6.
29. D. R. Do Carmo, D. S. Fernandes, L. R. Cumba, M. S. Magossi and V. S. Dos Santos, *Mater. Res. Bull.,* 84 (2016) 370.

30. L. A. Soares, W. Yingzi, T. F. S. Da Silveira, D. R. Silvestrini, U. O. Bicalho, N. L. Dias Filho and D. R. Do Carmo, *Int. J. Electrochem. Sci.,* 8 (2013) 7565.
31. D. R. Do Carmo, L. L. Paim, G. Metzker, N. L. Dias Filho and N. R. Stradiotto, *Mater. Res. Bull.,* 45 (2010) 1263.
32. D. R. Do Carmo, D. W. Franco, U. P. Rodrigues Filho, Y. Gushikem, E. Stadler and V. Drago, *J. Coord. Chem.,* 54 (2001) 455.
33. D. Engel and E. W.Grabner, *Ber. Bunsenges. Phys. Chem.,* 89 (1985) 982.
34. L. R. Cumba, U. O. Bicalho and D. R. Do Carmo, *Int. J. Electrochem. Sci.,* 7 (2012) 4465.
35. L. R. Cumba, U. O. Bicalho, D. R. Silvestrini and D. R. Do Carmo, *Int. J. Chem.,* 4 (2012) 66.
36. D. Jayasri and S. S. Narayanan, *Sens. Actuators B Chem.,* 119 (2006) 135.
37. A. R. F. Pipi and D. R. Do Carmo, *J. Appl. Electrochem.,* 7 (2011) 787.
38. A. J. Bard, L. R. Faulkner, *Electrochemical methods: Fundamentals and Applications*, John Wiley, New York, 2001.
39. T. F. S. Da Silveira, D. S. Fernandes, M. S. Magossi, P. F. P. Barbosa, T. R. Souza, M. S. Magossi and D. R. Do Carmo, *Int. J. Electrochem. Sci.,* 11 (2016) 7527.
40. T. R. Ralph, M. L. Hitchman, J. P. Millington and F. C. Walsh, *J. Electroanal. Chem.,* 375 (1994) 1.
41. W. Hou and E. Wang, *J. Electroanal. Chem. Interfacial Electrochem.,* 316 (1991) 155.
42. N. Spãtaru, B. V. Sarada, E. Popa, D.A. Tryk and A. Fujishima, *Anal. Chem.,* 73 (2001) 51